



OPEN

Enhancing CO₂ adsorption capacity of ZIF-8 by synergetic effect of high pressure and temperature

Shan Jiang¹, Jingyan Liu¹, Jiwen Guan², Xin Du³, Shoushun Chen³, Yang Song^{1,2}✉ & Yining Huang¹✉

Metal–organic frameworks (MOFs) and zeolitic imidazolate frameworks (ZIFs) are promising porous materials for adsorption and storage of greenhouse gases, especially CO₂. In this study, guided by the CO₂ phase diagram, we explore the adsorption behavior of solid CO₂ loaded with ZIF-8 framework by heating the sample under high pressures, resulting in a drastic improvement in the CO₂ uptake. The behavior of CO₂ under simultaneous high temperature (T) and pressure (P) conditions is directly monitored by in situ FTIR spectroscopy. The remarkable enhancement in CO₂ adsorption capability observed can be attributed to the synergetic effect of high T and P: high temperature greatly enhances the transport property of solid CO₂ by facilitating its diffusion into the framework; high pressure effectively modifies the pore size and shape via changing the linker orientation and creating new adsorption sites within ZIF-8. Our study thus provides important new insights into the tunability and enhancement of CO₂ adsorptive capability in MOFs/ZIFs using pressure and temperature combined as a synergetic approach.

To address the challenges associated with global warming, greenhouse gases and especially carbon dioxide capture and storage is of fundamental importance. Compared to the low energy efficient chemisorption-based methods, solid physisorbent materials such as activated carbons, zeolites, metal–organic frameworks (MOFs) and zeolitic imidazolate frameworks (ZIFs), which have lower heat capacities and require lower regeneration energy, have attracted increasing attention. In particular, MOFs and ZIFs as a subclass of MOFs have emerged as promising porous materials for greenhouse gas capture and storage. These materials have unique properties such as very high surface area, well defined porosity, high chemical and structural stability along with their modularity and tunable pore size/functionality^{1,2}. All these properties present remarkable potential for achieving optimal CO₂ capture and storage performance. In the large ZIF family, ZIF-8 [Zn(MeIm)₂, MeIm = 2-methylimidazolate] is the most well-known member. ZIF-8 is constructed by connecting each zinc ion tetrahedrally to four individual methylimidazolate ligands. It has a sodalite (SOD) topology containing the cages with a diameter of 11.6 Å and a cage aperture of 3.4 Å (Supplementary Fig. S1)³. These specific parameters make ZIF-8 to exhibit excellent adsorptive ability towards small gas molecules with appropriate kinetic diameters⁴, whose structural properties and gas adsorption performance including CO₂ have been extensively studied in the past decade under ambient conditions, high external pressures and at low temperatures by experimental and computational methods^{5–8}.

Recent investigations of pressure effect in different classes of MOFs are of particular interest which revealed highly diversified structural behaviours^{9–20}. Among these, ZIFs and especially ZIF-8 under high external pressure have been examined extensively^{21–28}. More significantly, several studies have shown that application of high external pressure can effectively tune CO₂ storage capability in MOFs/ZIFs^{8,29–32}. This is because external pressure can change the MOF/ZIFs framework topology, alter pore size and shape, enhance host–guest interactions between framework and adsorbed CO₂, and even create new adsorption sites, leading to an increased CO₂ adsorptive capability. However, at room temperature, solidification of CO₂ occurs at a pressure above 0.6 GPa³³. This phase change of CO₂ severely limits further insertion of CO₂ into the cavities of ZIF-8 at higher pressures since solid CO₂ is immobile and not diffusible. This problem can be remediated if a mixture of solid CO₂ and ZIF-8 is heated to a temperature at which solid CO₂ existing outside ZIF-8 is mobilized, so that a significantly larger number of CO₂ molecules may be pressed into the framework of ZIFs by pressure. More importantly, the detailed structural information, pressure and temperature stability, as well as the CO₂ adsorption properties in

¹Department of Chemistry, The University of Western Ontario, London, ON N6A 5B7, Canada. ²Department of Physics and Astronomy, The University of Western Ontario, London, ON N6A 5B7, Canada. ³College of Chemistry and Chemical Engineering, Lanzhou Magnetic Resonance Center, Lanzhou University, Lanzhou 730000, China. ✉email: yang.song@uwo.ca; yhuang@uwo.ca

ZIF-8 established in previous studies allows the understanding of the possible synergetic high-P and high-T effect on CO₂ adsorption in ZIF-8. In this work, using CO₂ phase diagram³³ as a guide and in situ IR spectroscopy as a tool, we examined CO₂ adsorption behaviour of ZIF-8 in a diamond-anvil cell (DAC) by simultaneously applying high temperature and pressure. To the best of our knowledge, this is the first report that investigates the CO₂ intake behaviour at simultaneous high-P and high-T conditions for MOFs and especially for ZIF-8. Our results clearly show that under the carefully controlled high P–T conditions, CO₂ uptake of ZIF-8 is enhanced drastically, making it a promising material for CO₂ storage.

Results

A typical IR spectrum of a mixture of CO₂ and activated (empty) ZIF-8 loaded into a DAC (hereafter referred to as CO₂/ZIF-8) under pressure (e.g., 1.02 GPa) along with the spectrum of activated ZIF-8 is shown in Fig. 1. The observation of very strong CO₂ fundamental modes, ν_2 and ν_3 , confirms that CO₂ was successfully loaded into the DAC. However, these peaks are too intense and saturated, preventing further data analysis. As shown in literature work^{34,35}, in such a situation, two CO₂ combination modes, ($\nu_3 + 2\nu_2$) and ($\nu_3 + \nu_1$) observed at around 3600 and 3710 cm⁻¹ in the IR spectra can be more effectively used to monitor the behaviour of adsorbed CO₂ inside porous framework^{29,30}. It is worth noting that at 1.02 GPa, each combination mode split into a doublet. The shape and position of the sharper high-frequency component for each mode are almost identical to those of pure CO₂, suggesting that it is due to the CO₂ outside the ZIF-8 framework in solid phase, whereas the broader low-frequency component is due to the CO₂ molecules that have entered the framework of ZIF-8 similar to that observed in other MOFs we reported previously^{29,30}. The relative intensity of these bands forms the basis for quantitative analysis of CO₂ in different environment under specific pressure and temperature conditions.

The selected variable temperature IR spectra of the CO₂ combination modes of the CO₂/ZIF-8 collected at a fixed pressure of 0.63 GPa are shown in Fig. 2a. At room temperature, each combination mode exhibits two components, indicating that the CO₂ molecules in the sample chamber experience two different environments. According to the CO₂ phase diagram³³, the CO₂ residing outside ZIF-8 should exist as a crystalline solid. As mentioned above, the high-frequency sharp component of each combination mode originates from the solid CO₂ outside the ZIF-8 framework. The CO₂ molecules adsorbed inside the framework of ZIF-8, on the other hand, give rise to the broader low-frequency component. At 36 °C, both the high-frequency components of ($\nu_3 + 2\nu_2$) and ($\nu_3 + \nu_1$) modes become less intense, while the low-frequency component of each mode becomes broader, suggesting that the solid CO₂ residing outside the framework undergoes a solid-to-fluid transition at current temperature and pressure. Markedly reduced intensity of the peak associated with solid CO₂ implies that a significant portion of the CO₂ that initially resides outside the framework at room temperature has now entered the framework at this temperature. Upon further heating at 40 °C, the intensity of the high-frequency component representing solid CO₂ vanishes completely, indicating that all the solid CO₂ initially residing outside the ZIF-8 framework has largely entered the framework due to the temperature enhanced fluidity. After cooling the DAC system down to room temperature, the higher frequency component of the doublet of both ($\nu_3 + 2\nu_2$) and ($\nu_3 + \nu_1$) modes reappears, but the intensity is much weaker compared to its low-frequency counterpart, suggesting that the CO₂ outside ZIF-8 recrystallizes upon cooling. This observation unambiguously indicates

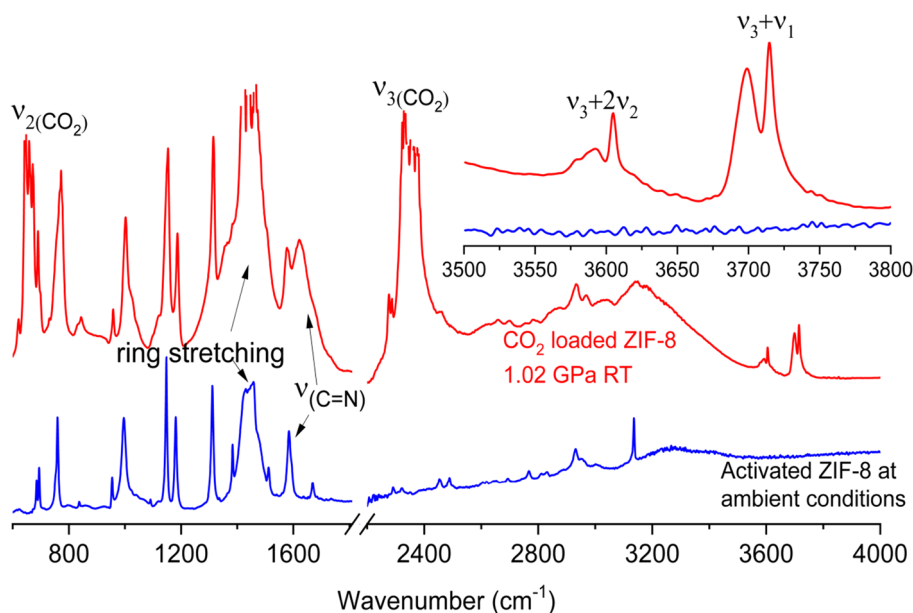


Figure 1. Mid-IR spectra of activated ZIF-8 at ambient pressure (blue) and CO₂ loaded ZIF-8 at 1.02 GPa (red). The inset shows the comparison between the activated (bottom) and CO₂ loaded ZIF-8 (top) in the spectral region of the CO₂ combination modes.

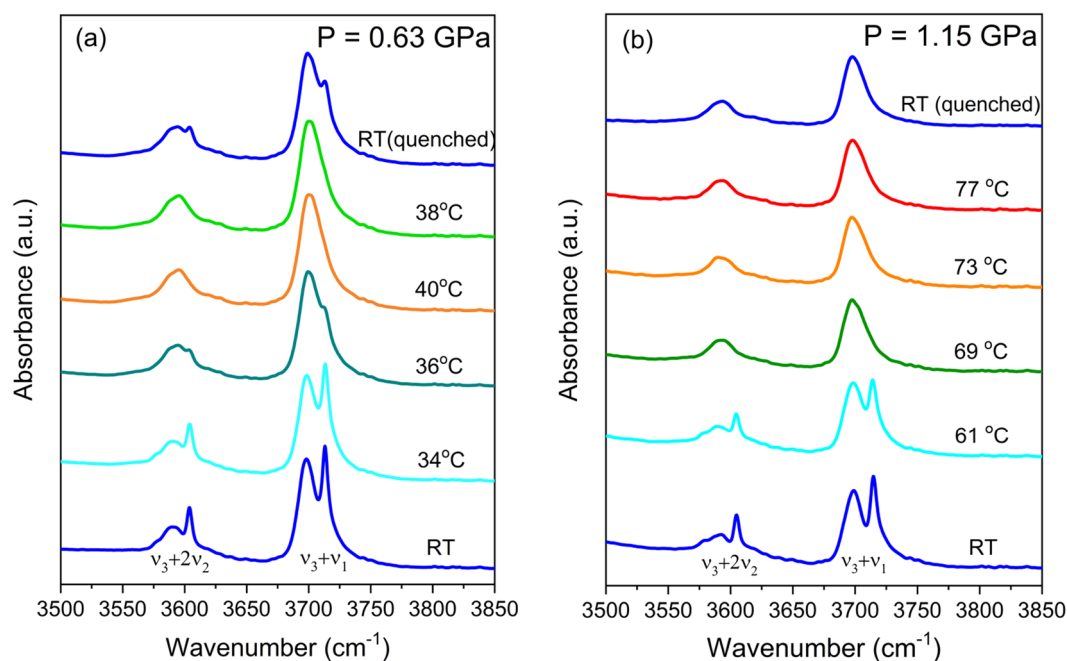


Figure 2. CO₂ adsorption capacity of ZIF-8 in percentage as a function of pressure and temperature. The data are obtained along a heating sequence at a fixed pressure followed by cooling (quenched) and analyzed using the characteristic combination IR mode of CO₂. A maximum enhancement (by 80%) of CO₂ adsorption by heating was achieved at 1.15 GPa (see text).

that after the heating cycle, the number of CO₂ molecules adsorbed inside ZIF-8 at room temperature is larger than that before heating. The ratio of CO₂ amount adsorbed inside the framework to those outside ZIF-8 can be estimated quasi-quantitatively from the integrated peak areas obtained by spectral deconvolution.

The two overlapping bands of the ($\nu_3 + \nu_1$) mode in each spectrum of the CO₂/ZIF-8 at different temperatures and under a fixed pressure of 0.63 GPa were deconvoluted (Supplementary Fig. S2) and the normalized peak areas are listed in Supplementary Table S1. Before heating, the fraction of CO₂ inside the ZIF-8 at room temperature is 55%; it then increases to 62% upon heating to 36 °C. At 40 °C, the normalized peak area representing CO₂ inside the framework reaches 78%, and the rest of the CO₂ remains as a fluid outside the framework (Supplementary Fig. S2). Upon cooling down to room temperature, the normalized peak area of the adsorbed CO₂ decreases to 62%. Thus, the amount of CO₂ adsorbed in the framework at room temperature and a pressure of 0.63 GPa increased by 13% compared to that before heating. It is thus apparent that simultaneously applying high temperature and pressure enhances ZIF-8's CO₂ adsorption capability. More importantly, a larger amount of CO₂ is trapped irreversibly inside the framework upon cooling to room temperature. Such permanent heating-enhanced CO₂ adsorption of ZIF-8 framework under a confined condition has not been observed for any other MOF materials to the best of our knowledge.

To further explore and optimize the synergetic effect of high pressure and high temperature on enhancing CO₂ uptake, additional variable temperature experiments at different pressures were also performed. The selected variable temperature IR spectra of the CO₂/ZIF-8 at a fixed pressure of 1.15 GPa are illustrated Fig. 2b. At 61 °C, the IR spectrum with sharp ($\nu_3 + 2\nu_2$) and ($\nu_3 + \nu_1$) modes clearly shows that CO₂ inside the sample chamber remains solid at this pressure. When heated to higher temperatures such as 69, 73 and 77 °C, all solid CO₂ appears melted with most of the CO₂ molecules transported into the framework of ZIF-8 by diffusion. Upon cooling from 77 °C down to room temperature, both ($\nu_3 + 2\nu_2$) and ($\nu_3 + \nu_1$) modes remain as a single broad peak, suggesting that no solid CO₂ phase is recovered. This result is significant as at room temperature and 1.15 GPa, any CO₂ existing outside ZIF-8 framework should be in solid phase. Among other additional CO₂ adsorption measurements following different P–T paths, we found that 1.15 GPa is close to an optimized pressure at which CO₂ adsorption enhancement is maximized upon heating to a temperature near the melting point of CO₂. Such a mild pressure–temperature condition can be readily realized in other devices such as multi-anvil press to allow scaling up. The normalized peak area (Supplementary Table S2) indicates that at 1.15 GPa and room temperature, 54% of the total CO₂ are initially adsorbed inside the cages of ZIF-8 and 46% of CO₂ resides outside the framework as a solid. Apparently upon heating followed by cooling back to room temperature, all the CO₂ molecules have now migrated and been trapped inside the ZIF-8 framework. A careful inspection reveals that upon cooling down to room temperature, the peak due to the ($\nu_3 + 2\nu_2$) mode has an asymmetric peak profile; the deconvoluted spectrum (Supplementary Fig. S3) shows a small broad peak with a Gaussian profile at the high-frequency side of the main peak, indicating that there are two non-equivalent CO₂ inside ZIF-8 (see discussion below). The heat treatment at 1.15 GPa leads to an 85% increase in the amount of adsorbed CO₂ in ZIF-8, compared to only 13% enhancement of CO₂ uptake under 0.63 GPa. We further explored the CO₂ uptake behaviour in ZIF-8

framework under other P–T conditions extensively (up to 2.4 GPa and over 145 °C) and found 1.15 GPa is the closest to an optimal pressure under which the heating-enhanced CO₂ adsorption achieves the maximum. These findings are summarized in Fig. 3.

Discussion

The substantial difference in adsorptive capacity improvement under different pressures is intriguing and can be closely attributed to the framework structure under different pressures and temperatures. Previous work by Moggach et al.²¹ showed that high external pressure can increase the effective pore size of ZIF-8 by changing the linker orientation, which is so called “gate opening” effect. Hobday et al. further established a correlation between the pressure and the rotation angle (θ) of the imidazole rings describing the pore opening (Fig. 4)²⁶. Such rotation of the linker results in an increase in the unit cell volume and solvent-accessible volume^{6,26}. In the present case, it appears that at 0.63 GPa, the pressure is not high enough to fully rotate the imidazole ring to open the gate completely. Consequently, at this pressure, the CO₂ uptake has not reached the maximum even though the fluidity of CO₂ is significantly enhanced by heating. The work by Moggach et al.²¹ elegantly demonstrated that ZIF-8 transforms to a new phase at 1.47 GPa (a pressure close to 1.15 GPa explored in this study) where both the pore volume and the size of the linking channels increase. At 69 °C and 1.15 GPa, we believe that the small and broad high-frequency peak in the deconvoluted spectrum (Supplementary Fig. S3) represents 22% of CO₂ molecules that are adsorbed in the channels surrounding each sodalite cage and are distinctively different than those 78% in the cages. These channels are otherwise blocked by imidazole linkers and not accessible at the ambient pressure. The CO₂ molecules adsorbed in the channels are tightly confined compared to those inside the cages. Consequently, the CO₂ vibrations appeared at higher frequencies due to the strong confinement. The fact that no solid phase of CO₂ reforms upon cooling down to room temperature implies that all the CO₂ molecules are trapped tightly inside ZIF-8 due to the strong interaction of CO₂ with the framework under pressure. The combined pressure–temperature effect on the structural details of ZIF-8 framework is illustrated in Fig. 4.

To further confirm that fluidity of CO₂ under applied pressure by heating is critically important to the large enhancement of CO₂ uptake of ZIF-8, we heated the CO₂/ZIF-8 mixture in a DAC at temperature up to above 145 °C under a higher pressure of 2.41 GPa. CO₂ phase diagram shows that the free CO₂ residing outside the framework should remain as a solid in the entire T, P range employed. Indeed, the high-frequency component of the ($\nu_3 + \nu_1$) mode representing solid CO₂ persists in the spectra throughout the entire temperature range (Supplementary Fig. S4). No CO₂ uptake enhancement was observed either during heating or upon cooling down to room temperature (Supplementary Fig. S4). These results unambiguously indicate that neither heating solid CO₂ nor applying pressure alone can sufficiently improve the CO₂ adsorptive capability of ZIF-8. Careful inspection of the room temperature spectra acquired at 2.41 GPa before and after heating reveals that the intensity of the high-frequency peak corresponding to solid CO₂ actually becomes slightly stronger with respect to the low-frequency component due to the CO₂ inside ZIF-8, implying that the CO₂ adsorptive ability is slightly reduced after the heat treatment (Supplementary Fig. S4). A possible reason is that the framework might have been partially damaged by exposing the ZIF-8 to harsher conditions (i.e. 2.41 GPa and 145 °C), resulting in a slightly reduced porosity for adsorption. The quantitative CO₂ intake enhancement and detailed CO₂ adsorption

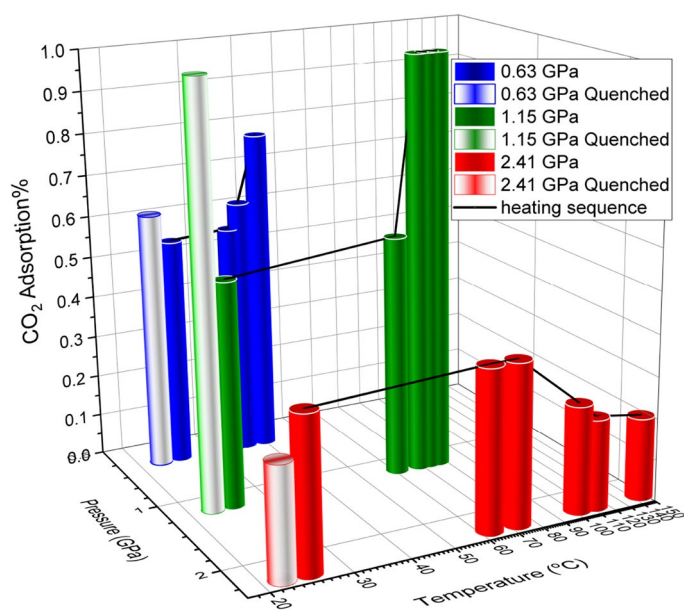


Figure 3. CO₂ adsorption capacity of ZIF-8 in percentage as a function of pressure and temperature. The data are obtained along a heating sequence at a fixed pressure followed by cooling (quenched) and analyzed using the characteristic combination IR mode of CO₂. A maximum enhancement (by 80%) of CO₂ adsorption by heating was achieved at 1.15 GPa (see text).

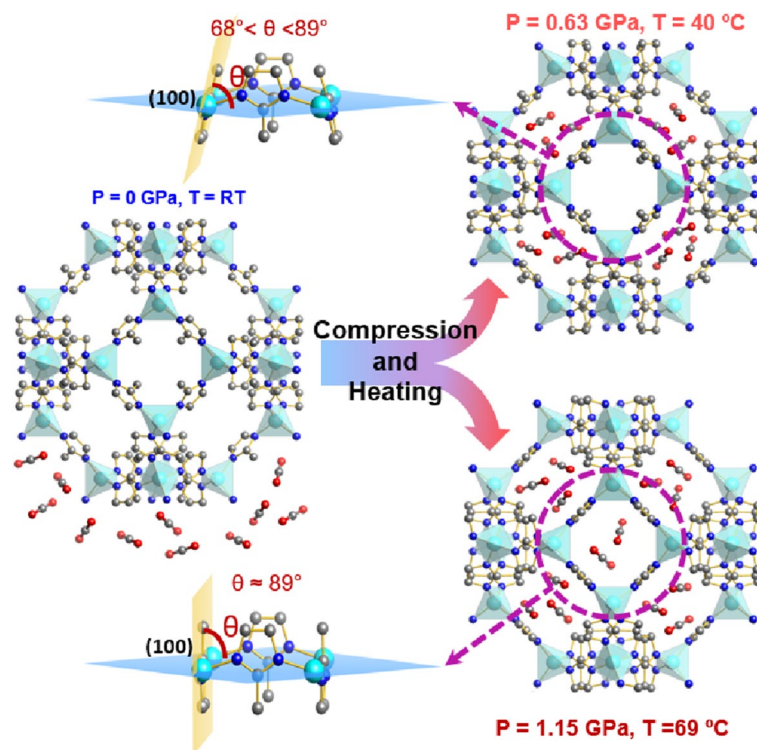


Figure 4. Schematics of CO₂ adsorption and structural change in the CO₂ loaded ZIF-8 framework from near ambient pressure and room temperature (left) to 0.63 GPa and 40 °C (upper right) and to 1.15 GPa and 69 °C (lower right). The pressure-dependent “gate” opening effect is illustrated by the rotation angle of the methylimidazole rings (see text).

mechanism at simultaneously high P–T conditions should be verified by synchrotron single crystal diffraction measurements as well as computational modelling in the future. Moreover, whether the synergetic P–T effect is applicable to other MOFs in different classes invites more systematic study on other MOFs.

Conclusions

In summary, using in situ IR spectroscopy, we demonstrate that simultaneously applying moderate temperature and pressure to a CO₂/ZIF-8 mixture can remarkably enhance the CO₂ adsorptive capacity of ZIF-8. Specifically, the thermal treatment was applied simultaneously at high pressures up to 2.41 GPa. The optimized T, P condition established in this study is 69 °C and 1.15 GPa, under which an 85% increase in CO₂ uptake is achieved. Such a drastic enhancement of CO₂ adsorption ability is attributed to the synergetic effect of high T and P. High temperature significantly enhances the transport property of CO₂, allowing CO₂ to effectively diffuse into the framework of ZIF-8. Meanwhile, high mechanical pressure changes the effective pore size and shape as well as the linker orientation to open the “gate”, facilitating the CO₂ adsorption. The change in the linker orientation also makes the channels connecting the cages accessible to CO₂ as additional adsorption sites at high pressure. This work demonstrates that gas adsorption capability of MOFs and ZIFs can be drastically improved by applying moderate pressure and temperature, making ZIFs a promising class of materials for practical CO₂ storage applications.

Methods

ZIF-8 was synthesized solvothermally and activated by following the literature method³⁶. Briefly, A mixture of 2.5 mmol Zn(NO₃)₂·6H₂O (Alfa Aesar, 98%) and 0.15 mol 2-methylimidazole (Sigma-Aldrich, 98%) were dissolved in 100 mL of deionized water and stirred at room temperature for 24 h. The resulting white crystals were harvested via vacuum filtration and washed with 10 mL of methanol for three times. Activation of ZIF-8 samples was achieved by degassing via dynamic vacuum and heating for 8 h at 150 °C. The identity and purity of the activated product were verified by powder X-ray diffraction (PXRD) to show the successful removal of the solvent to achieve an activated (empty) ZIF-8 framework. (Supplementary Fig. S5). The PXRD pattern was recorded using a Inel CPS X-ray diffractometer operating with Cu K α radiation ($\lambda = 1.5406 \text{ \AA}$). The reflections were collected at 2θ values ranging between 5 and 40°, using an increment of 0.01° with an acquisition rate of 4°/min. Thermogravimetric Analysis (TGA) measurements were performed by Beijing HENVEN HQT-3 instrument. The sample was heated from 25° to 800 °C at a rate of 10 °C/min under a N₂ atmosphere. The TGA profile of the activated sample (Supplementary Fig. S6) shows no weight loss below around 600 °C, which clearly indicates that all the solvent molecules were removed during activation process and the activation is complete. The weight loss at the temperature above 600 °C is due to the decomposition³⁶, indicating the ZIF-8 is stable up to c.a. 600

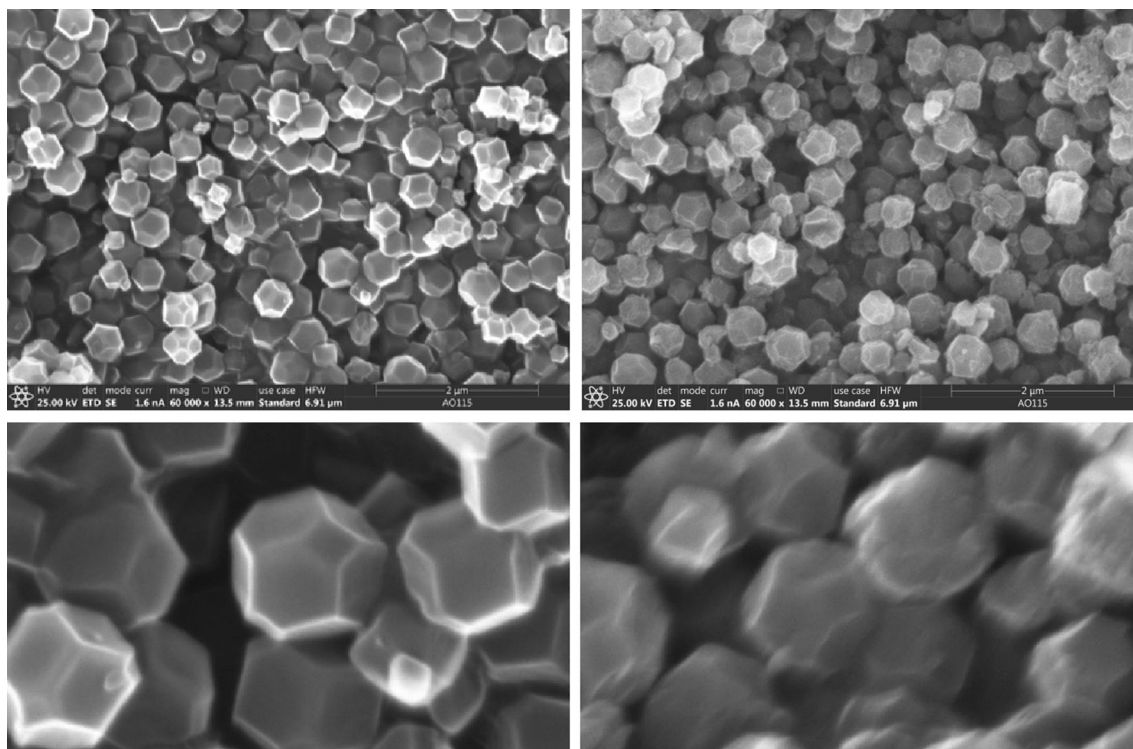


Figure 5. SEM images of as-made (left column) and activated (right column) ZIF-8 samples at different magnifications.

°C. Scanning Electron Microscopy (SEM) measurements were conducted using a Thermo Scientific Apreo S SEM instrument operating at 30 kV. SEM images of as-made and activated ZIF-8 samples are shown in Fig. 5. ZIF-8 crystals display a consistent truncated octahedral shape with uniform particle dimensions, in agreement with previously reported studies³⁶. The surface area of activated ZIF-8 was measured using BET method with a BELSORP-MAX instrument with N₂ (99.999%) at 77 K. Prior to N₂ isotherm measurement, 100 mg of ZIF-8 was achieved by degassing via dynamic vacuum and heating for 8 h at 150 °C. N₂ adsorption experiments at pressures up to 1 bar was then performed on activated ZIF-8 by the BELSORP-MAX. The N₂ adsorption isotherms measured for activated ZIF-8 sample is shown in Supplementary Fig. S7. The BET area derived is 1686.7 m²/g, surpassing the best value (i.e., 1550 m²/g) reported in a previous literature³⁶, indicating the successful activation and excellent porosity of ZIF-8 achieved in this study.

To carry out in situ high T-P experiments, a DAC (Supplementary Fig. S8) equipped with a pair of type II diamonds (600 μm culet size) was used for all IR measurements. The sample chamber was prepared on a stainless-steel gasket, with 60–80 μm in thickness and 300 μm in diameter. A few ruby chips were pre-loaded into the sample chamber for pressure calibration³⁷. For sample preparation, in order to maximize the CO₂ loading, the sample chamber was firstly half filled with activated (empty) ZIF-8. The piston side of the DAC was then immersed in a liquid nitrogen bath to cool down the system. During this process, the sample chamber was covered with a plastic film to avoid moisture condensation. When the temperature of the gasket was below the melting point of dry ice (i.e., < 78.5 °C), the plastic film was removed, and the CO₂ gas was introduced into the sample chamber. Upon closing the DAC, a low pressure is needed to hold CO₂ in the sample chamber for further measurements. The FTIR spectrometer used is customized for in situ high pressure measurements, with the details described in previous publications³⁸. In this work, to apply high pressure and high temperature simultaneously and take IR measurement in situ, the regular DAC stage for room temperature measurement was replaced by a custom-designed heating stage, which is composed of a resistively heated copper cell holder, and a glass wool board for heat insulation. By placing the DAC onto this stage, high temperature (up to ~ 500 °C) could be achieved by powering up the heating element with AC current from a power supply with a temperature controller (omega iSeries) to regulate the heat delivery and to control the temperature of the DAC. Temperature is measured by attaching a calibrated thermocouple to the back of the diamond. The accuracy of the temperature measurement is ± 2.3 °C in the temperature range from 50–80 °C and ± 5.0 °C from 80 to 200 °C.

Data availability

All data generated or analysed during this study are either included in this published article and its supplementary information files or are available from the corresponding author on reasonable request.

Received: 8 August 2023; Accepted: 13 October 2023

Published online: 16 October 2023

References

- Wang, B., Cote, A. P., Furukawa, H., O’Keeffe, M. & Yaghi, O. M. Colossal cages in zeolitic imidazolate frameworks as selective carbon dioxide reservoirs. *Nature* **453**, 207–211 (2008).
- Phan, A. *et al.* Synthesis, structure, and carbon dioxide capture properties of zeolitic imidazolate frameworks. *Acc. Chem. Res.* **43**, 58–67 (2010).
- Banerjee, R. *et al.* High-throughput synthesis of zeolitic imidazolate frameworks and application to CO₂ capture. *Science* **319**, 939–943 (2008).
- Perez-Pellitero, J. *et al.* Adsorption of CO₂, CH₄, and N₂ on zeolitic imidazolate frameworks: experiments and simulations. *Chem. Eur. J.* **16**, 1560–1571 (2010).
- Fairen-Jimenez, D. *et al.* Flexibility and swing effect on the adsorption of energy-related gases on ZIF-8: combined experimental and simulation study. *Dalton Trans.* **41**, 10752–10762 (2012).
- Fairen-Jimenez, D. *et al.* Opening the gate: framework flexibility in ZIF-8 explored by experiments and simulations. *J. Am. Chem. Soc.* **133**, 8900–8902 (2011).
- Pantatosaki, E. *et al.* On the impact of sorbent mobility on the sorbed phase equilibria and dynamics: a study of methane and carbon dioxide within the zeolite imidazolate framework-8. *J. Phys. Chem. C* **116**, 201–207 (2011).
- Hu, Y., Liu, Z., Xu, J., Huang, Y. & Song, Y. Evidence of pressure enhanced CO₂ storage in ZIF-8 probed by FTIR spectroscopy. *J. Am. Chem. Soc.* **135**, 9287–9290 (2013).
- Gagnon, K. J., Beavers, C. M. & Clearfield, A. MOFs under pressure: the reversible compression of a single crystal. *J. Am. Chem. Soc.* **135**, 1252–1255 (2013).
- Graham, A. J. *et al.* Stabilization of scandium terephthalate MOFs against reversible amorphization and structural phase transition by guest uptake at extreme pressure. *J. Am. Chem. Soc.* **136**, 8606–8613 (2014).
- Ortiz, A. U., Boutin, A., Gagnon, K. J., Clearfield, A. & Coudert, F. X. Remarkable pressure responses of metal-organic frameworks: proton transfer and linker coiling in zinc alkyl gates. *J. Am. Chem. Soc.* **136**, 11540–11545 (2014).
- Spencer, E. C. *et al.* Pressure-induced bond rearrangement and reversible phase transformation in a metal-organic framework. *Angew. Chem. Int. Ed.* **53**, 5583–5586 (2014).
- Su, Z., Miao, Y. R., Zhang, G., Miller, J. T. & Suslick, K. S. Bond breakage under pressure in a metal organic framework. *Chem. Sci.* **8**, 8004–8011 (2017).
- Mao, H., Xu, J., Hu, Y., Huang, Y. & Song, Y. The effect of high external pressure on the structure and stability of MOF α -Mg₅(HCOO)₆ probed by in situ Raman and FT-IR spectroscopy. *J. Mater. Chem. A* **3**, 11976–11984 (2015).
- Widmer, R. N. *et al.* Pressure promoted low-temperature melting of metal-organic frameworks. *Nat. Mater.* **18**, 370–376 (2019).
- Celeste, A. *et al.* Mesoporous metal-organic framework MIL-101 at high pressure. *J. Am. Chem. Soc.* **142**, 15012–15019 (2020).
- Robison, L. *et al.* Designing porous materials to resist compression: mechanical reinforcement of a Zr-MOF with structural linkers. *Chem. Mater.* **32**, 3545–3552 (2020).
- Polrolniczak, A. & Katrusiak, A. Self-healing ferroelastic metal-organic framework sensing guests, pressure and chemical environment. *Mater. Adv.* **2**, 4677–4684 (2021).
- Troyano, J., Legrand, A. & Furukawa, S. Mechanoresponsive porosity in metal-organic frameworks. *Trends Chem.* **3**, 254–265 (2021).
- Vervoorts, P. *et al.* Configurational entropy driven high-pressure behaviour of a flexible metal-organic framework (MOF). *Angew. Chem. Int. Ed.* **60**, 787–793 (2021).
- Moggach, S. A., Bennett, T. D. & Cheetham, A. K. The effect of pressure on ZIF-8: increasing pore size with pressure and the formation of a high-pressure phase at 1.47 GPa. *Angew. Chem. Int. Ed.* **48**, 7087–7089 (2009).
- Spencer, E. C., Angel, R. J., Ross, N. L., Hanson, B. E. & Howard, J. A. Pressure-induced cooperative bond rearrangement in a zinc imidazolate framework: a high-pressure single-crystal X-ray diffraction study. *J. Am. Chem. Soc.* **131**, 4022–4026 (2009).
- Bennett, T. D. *et al.* Reversible pressure-induced amorphization of a zeolitic imidazolate framework (ZIF-4). *Chem. Commun.* **47**, 7983–7985 (2011).
- Hu, Y., Kazemian, H., Rohani, S., Huang, Y. & Song, Y. In situ high pressure study of ZIF-8 by FTIR spectroscopy. *Chem. Commun.* **47**, 12694–12696 (2011).
- Im, J., Yim, N., Kim, J., Vogt, T. & Lee, Y. High-pressure chemistry of a zeolitic imidazolate framework compound in the presence of different fluids. *J. Am. Chem. Soc.* **138**, 11477–11480 (2016).
- Hobday, C. L. *et al.* Understanding the adsorption process in ZIF-8 using high pressure crystallography and computational modelling. *Nat. Commun.* **9**, 1429 (2018).
- Chen, S. L. *et al.* Intrinsic and extrinsic responses of ZIF-8 under high pressure: a combined Raman and X-ray diffraction investigation. *J. Phys. Chem. C* **123**, 29693–29707 (2019).
- Erkartal, M. & Durandurdu, M. Pressure-induced amorphization, mechanical and electronic properties of zeolitic imidazolate framework (ZIF-8). *Mater. Chem. Phys.* **240**, 122222 (2020).
- Hu, Y. *et al.* Probing the structural stability of and enhanced CO₂ storage in MOF MIL-68(In) under High pressures by FTIR spectroscopy. *Chem. Eur. J.* **21**, 18739–18748 (2015).
- Jiang, S., Hu, Y., Chen, S., Huang, Y. & Song, Y. Elucidation of the structural origins and contrasting guest-host interactions in CO₂-loaded CdSDB and PbSDB metal-organic frameworks at high pressures. *Chem. Eur. J.* **24**, 19280–19288 (2018).
- Choi, J. *et al.* Universal gas-uptake behavior of a zeolitic imidazolate framework ZIF-8 at high pressure. *J. Phys. Chem. C* **123**, 25769–25774 (2019).
- Kontos, A. G. *et al.* Correlating vibrational properties with temperature and pressure dependent CO₂ adsorption in zeolitic imidazolate frameworks. *Appl. Surf. Sci.* **529**, 147058 (2020).
- Giordano, V. M., Datchi, F. & Dewaele, A. Melting curve and fluid equation of state of carbon dioxide at high pressure and high temperature. *J. Chem. Phys.* **125**, 054504 (2006).
- Aoki, K., Yamawaki, H. & Sakashita, M. Phase study of solid CO₂ to 20 GPa by infrared-absorption spectroscopy. *Phys. Rev. B: Condens. Matter* **48**, 9231–9234 (1993).
- Santoro, M. *et al.* Silicon carbonate phase formed from carbon dioxide and silica under pressure. *Proc. Natl. Acad. Sci. U. S. A.* **108**, 7689–7692 (2011).
- Kida, K. *et al.* Formation of high crystalline ZIF-8 in an aqueous solution. *CrystEngComm* **15**, 1794–1801 (2013).
- Mao, H. K., Xu, J. & Bell, P. M. Calibration of the ruby pressure gauge to 800 kbar under quasi-hydrostatic conditions. *J. Geophys. Res.* **91**(B5), 4673 (1986).
- Dong, Z. & Song, Y. Transformations of cold-compressed multiwalled boron nitride nanotubes probed by infrared spectroscopy. *J. Phys. Chem. C* **114**, 1782 (2010).

Acknowledgements

Y.H. and Y.S. acknowledge the Natural Science and Engineering Research Council of Canada (NSERC) for Discovery Grants. An NSERC Discovery Accelerator Award (Y.H.), a Leading Opportunity Fund from the Canadian Foundation for Innovation (Y.S.) are also gratefully acknowledged.

Author contributions

Conceptualization: Y.H. and Y.S.; experimental and data processing: S.J., J.G., J.L., X.D. and S.C.; supervision: Y.H. and Y.S.; manuscript editing: Y.H. and Y.S. All authors contributed to the analysis and preparation of the manuscript.

Competing interests

The authors declare no competing interests.

Additional information

Supplementary Information The online version contains supplementary material available at <https://doi.org/10.1038/s41598-023-44960-4>.

Correspondence and requests for materials should be addressed to Y.S. or Y.H.

Reprints and permissions information is available at www.nature.com/reprints.

Publisher's note Springer Nature remains neutral with regard to jurisdictional claims in published maps and institutional affiliations.



Open Access This article is licensed under a Creative Commons Attribution 4.0 International License, which permits use, sharing, adaptation, distribution and reproduction in any medium or format, as long as you give appropriate credit to the original author(s) and the source, provide a link to the Creative Commons licence, and indicate if changes were made. The images or other third party material in this article are included in the article's Creative Commons licence, unless indicated otherwise in a credit line to the material. If material is not included in the article's Creative Commons licence and your intended use is not permitted by statutory regulation or exceeds the permitted use, you will need to obtain permission directly from the copyright holder. To view a copy of this licence, visit <http://creativecommons.org/licenses/by/4.0/>.

© The Author(s) 2023